Available online at www.sciencedirect.com
SCIENCE DIRECT®
Physica B 335 (2003) 44–49
PHYSICA B
www.elsevier.com/locate/physb

Polarized neutron reflectivity studies of magnetic semiconductor superlattices

H. Kępa[a,b,*], C.F. Majkrzak[c], A.Yu. Sipatov[d], T.M. Giebultowicz[b]

[a] *Institute of Experimental Physics, Warsaw University, ul. Hoża 69, 00-681 Warszawa, Poland*
[b] *Physics Department, Oregon State University, 301 Weniger Hall, Corvallis, OR 97331, USA*
[c] *NIST Center for Neutron Research, National Institute of Standards and Technology, Gaithersburg, MD 20899, USA*
[d] *Kharkov State Polytechnic University, 21 Frunze St., Kharkov 310002, Ukraine*

Abstract

Polarized neutron reflectivity studies of EuS/PbS, EuS/YbSe and GaMnAs/GaAs superlattices performed at the NIST Center for Neutron Research are presented. Pronounced antiferromagnetic (AFM) interlayer coupling has been found in EuS/PbS superlattices for a very broad range of PbS spacer thicknesses. Similar, but weaker, AFM coupling is also present in EuS/YbSe, although only for relatively thin YbSe layers. Neutron polarization analysis shows distinct in-plane asymmetry of the magnetization directions of EuS layers in both systems under investigation.

For GaMnAs/GaAs superlattices, ferromagnetic (FM) interlayer correlations have been observed. Polarized neutron reflectometry investigations of several GaMnAs/GaAs superlattices have revealed that the manganese magnetic moments in individual GaMnAs layers, in spite of low Mn concentration, form a truly long range, that is in certain cases a single domain, ferromagnetic state.
© 2003 Elsevier Science B.V. All rights reserved.

Keywords: Ferromagnetic semiconductors; Superlattices; Neutron reflectometry

1. Introduction

With the advent of spintronics, a novel branch of electronics where not only the charge of the carrier but also its spin plays a major role [1], there is a growing effort towards studies of semiconductor-magnetic nanostructures. The research is driven by numerous potential practical applications as well as by more fundamental scientific goals. Hybrid structures composed of semiconductors and ferromagnetic (FM) metals are one group of such devices, but even more interesting possibilities can be envisioned with nanostructures in which the FM metal component could be replaced by an appropriate FM semiconductor. There has been observed a variety of remarkable phenomena coming from the interplay between FM cooperative phenomena and semiconducting properties such as the change of magnetic phase isothermally by light or by the electric field in InMnAs/AlGaSb and the injection of spin-polarized carriers from GaMnAs to InGaAs quantum wells in the absence of an external magnetic field. In FM semiconductors, one can also demonstrate the presence of

*Corresponding author. Institut of Experimental Physics, Hoża 69, Warsaw 00-681, Poland. Fax: +48-22-629-4229.
E-mail address: henryk.kepa@fuw.edu.pl (H. Kępa).

0921-4526/03/$ - see front matter © 2003 Elsevier Science B.V. All rights reserved.
doi:10.1016/S0921-4526(03)00188-1

such phenomena, characteristic for metallic multilayers, as exchange interlayer coupling, exchange bias, giant and tunneling magnetoresistance. A recent comprehensive review on FM semiconductors, with a very extensive list of references to original papers, can be found in Ref. [2]. Understanding the ferromagnetism of these compounds is crucial for developing functional semiconductor devices. Here we present the results of polarized neutron reflectometry studies performed on a number of all-semiconductor FM/nonmagnetic superlattices.

2. EuS/YbSe superlattices

In earlier investigations, by unpolarized neutron diffraction and reflection, pronounced antiferromagnetic (AFM) interlayer coupling (IC) in EuS/PbS superlattices (SL) has been discovered [3]. The nature of the origin of this coupling is still not fully understood. Tight-binding model calculations point to the possibility of conveying the IC, especially at thinner ($d_{PbS} < 25$ Å) PbS spacers, by valence electrons in the system [4]. Another plausible explanation applicable for much thicker nonmagnetic spacers involves magnetic dipolar coupling. Similar IC has recently been found in another system, EuS/YbSe, although the strength and the range of the interlayer interaction in this case are considerably lower.

Polarized neutron reflectometry enables us to investigate the directional characteristics of the layer magnetization, e.g. the magnetic domain populations with respect to crystallographic in-plane directions.

In this section, we will concentrate on the results obtained for one sample, [EuS(46 Å)/YbSe(20 Å)] × 15, but very similar results were obtained in other samples too. At first, the X-ray reflectivity profile was taken to determine the structure of the superlattice. The result is shown in Fig. 1. The continuous line represents the reflectivity calculated by a procedure similar to that described by Parratt [5]. To get the best fit, a broadening (FWHM = 10 Å, i.e. ~3 monolayers) of the EuS–YbSe interfaces has to be assumed; it was also necessary to change the X-ray scattering length densities (SLD) of the constituent materials by about 10% from their bulk values. The latter may reflect the presence of some interdiffusion in the sample. A portion of the resulting SLD profile used in the calculation is shown in the inset of Fig. 1. In the subsequent analysis of polarized and unpolarized neutron reflectivities, the same EuS–YbSe interface structure and analogous changes to the bulk nuclear SLDs were applied.

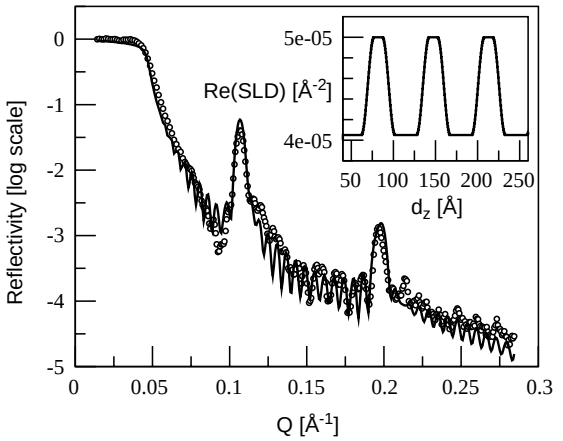

Fig. 1. X-ray reflectivity from EuS(46 Å)/YbSe(20 Å) × 15 superlattice. Shown in the inset is a portion of the X-ray Re(SLD), used in the calculation of the model reflectivity (—).

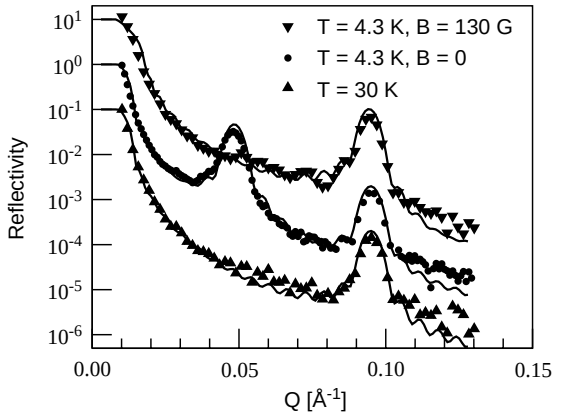

Fig. 2. Unpolarized neutron reflectivities for the EuS(46 Å)/YbSe(20Å) × 15 SL. Calculated reflectivity curves (—) are explained in the text.

The results of the unpolarized neutron reflectivity experiments on the same sample are summarized in Fig. 2. The data taken at 30 K, well above

the Curie temperature ($T_C = 18.5$ K), correspond only to nuclear scattering associated with the chemical structure of the superlattice at the first-order SL Bragg peak. Low-temperature data taken at 4.3 K, and in zero external magnetic field, show the characteristic, half-order AFM interlayer correlation. The half-order peak disappears under the influence of a sufficiently strong applied magnetic field, which aligns domains, overcoming the weak AFM interlayer coupling. The intensity of the first-order maximum increases due to the ferromagnetic contribution to the scattering, but this increase is smaller than that one should expect from the full saturation moment of the bulk EuS. As follows from the fit of the calculated reflectivity, the corresponding magnetic SLD is only 2.95×10^{-6} instead of 3.55×10^{-6} Å^{-2} derived from the bulk EuS saturation magnetization. Only part of this decrease can be attributed to YbSe interdiffusion into the EuS layer (seen in the 10% change of the nuclear SLDs). Some of the remaining missing moment might come from magnetically disordered Eu atoms in the vicinity of imperfect EuS–YbSe interface. As can be seen in Fig. 2, all the calculated reflectivities, represented by the continuous lines, fit the experimental points very well. The discussion of the curve for the low-temperature data in zero field will be postponed until the presentation of the polarized data results below.

In Fig. 3, the results of polarization analysis of the reflected neutron beam from the EuS(46 Å)/YbSe(20 Å) × 15 SL are presented. The non-spin-flip (NSF) cross sections are shown in part (a) and the spin-flip (SF) ones in part (b) of Fig. 3. The first-order structural Bragg SL peak is entirely NSF and there is no splitting between R^{++} and R^{--} reflectivities due to the interference between nuclear and magnetic scattering. Thus the first-order peak is purely nuclear in origin and no FM component due to possible interlayer correlations is present. This corroborates the unpolarized beam measurement, where there were no intensity differences below and above T_C. The purely magnetic half-order AFM maximum is predominantly SF, the ratio of SF intensity to NSF being about 5:1. This ratio may be indicative of domain magnetizations being at some finite angle to the horizontal axis. The solid lines in Fig. 3 represent the best fit of calculated reflectivities assuming this angle to be 0.4 rad with the magnetic SLD equal to 1.63×10^{-6} Å^{-2}. The latter value is significantly lower than 2.95×10^{-6} Å^{-2} derived from the saturation EuS layer magnetization (see unpolarized beam data taken at 130 G), one possible explanation being that within the lateral coherence length of the neutron beam (~ 100 μm), apart from some large domains with sizes comparable or bigger than the coherence length, there are many smaller domains, oriented in opposite directions, whose magnetizations average to zero. Thus, the smaller ones do not contribute to the specularly reflected intensity, thereby resulting in diminished observed magnetic SLD. The effect of mutual interplay of domain sizes and the lateral coherence length is shown schematically in Fig. 4.

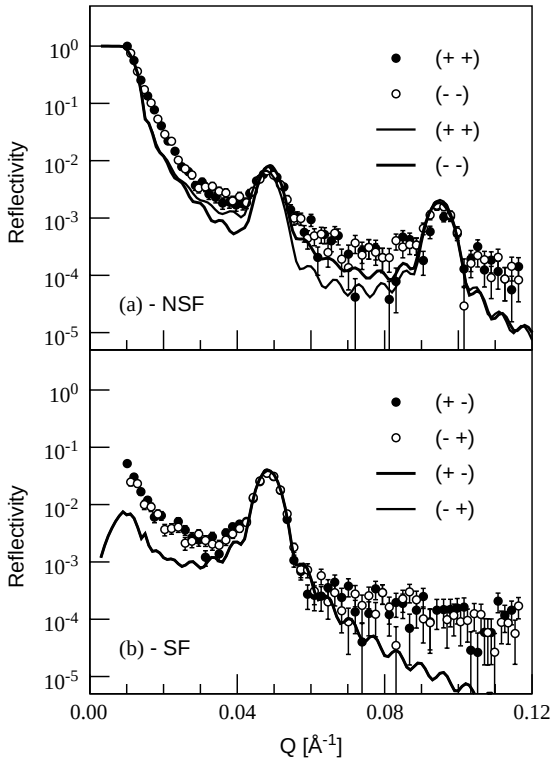

Fig. 3. (a) Non-spin-flip and (b) spin-flip polarized neutron reflectivities for the EuS(46 Å)/YbSe(20 Å) × 15 SL.

The calculated curves fit the experimental data very well within the Bragg SL peaks; the

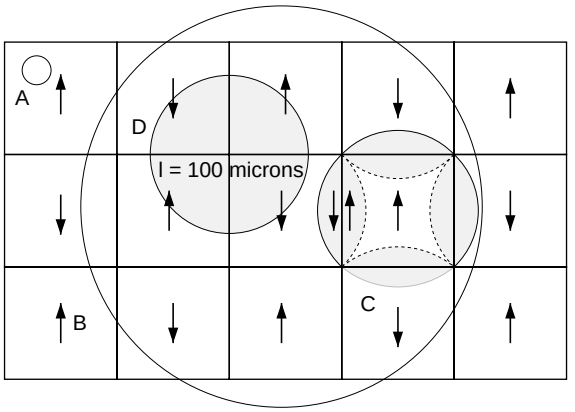

Fig. 4. The influence of magnetic domain size on reflected neutron intensity. Case A, very large domains compared to the lateral coherence length (LCL) represented schematically by the circle; the full magnetization is visible to the neutron. In case B, the domains are much smaller than LCL; most of the magnetization 'seen' by the neutron averages to about zero. If the domain size is comparable to LCL (case C), only part (unshaded) of the full domain magnetization contributes to the coherently reflected intensity. Near the domain boundary (case D), the area belonging to different domains effectively cancels out to zero.

discrepancies at very small Q are due to the influence of the incident beam; at large Q, where the reflectivity is relatively low, the experimental data is affected strongly by the background.

By addition of all the four polarized neutron reflectivities, one can obtain the reflectivity measured with the unpolarized beam. The quantity $0.5\times(R^{++}+R^{+-})+0.5\times(R^{--}+R^{-+})$ has been plotted in Fig. 2 and shows excellent agreement with the experimental points (4.3 K, $B=0$ G) obtained over the full range of momentum transfer. The unpolarized experiment was carried out with a much higher counting rate providing better accuracy. This comparison may serve as an additional test of our model reflectivity calculations for polarized cross sections.

During the polarized neutron analysis experiments, the sample [1 1 0] in-plane axis was placed in the horizontal direction. The easy axis along which the EuS layer magnetization is aligned lies very close, or very likely coincides with the [2 1 0] in-plane crystallographic direction which makes an angle of 0.32 rad with the [1 1 0] axis (the difference of 0.08 rad may be attributed to a small inaccuracy in the sample mounting).

Another possibility that cannot be ruled out, without additional measurements with the sample rotated about **Q**, is the presence of a fraction of domains having other orientations.

3. GaMnAs/GaAs system

Whereas EuS, with a relatively low T_C, belongs to a rare group of naturally occuring FMS, GaMnAs is a man-made diluted magnetic semiconductor (DMS) with a T_C approaching 110 K. Recent progress in the MBE growth of III–V-type DMS (such as GaMnAs, InMnAs, GaMnN) [6] raised hopes for a 'good' spintronics material. The Curie points of these materials are still much below room temperature, which limits their practicality. Nevertheless, they may play an important role in developing prototypes of future spintronic devices.

The most desirable situation from the spintronics viewpoint is spontaneous formation of a single-domain FM state, thus reducing the need for an external applied magnetic field. Our current picture of the domain structure of the new epitaxial ferromagnets is still incomplete. In general, the present knowledge of GaMnAs ferromagnetism is based on magnetization and transport measurements, which probe only the volume properties of the spin system.

By applying the technique of polarization analysis, we were able to observe the magnetic scattering contributions from domain states. The results show that in most samples, cooling through the Curie temperature in zero external field leads to the formation of *single-domain* ferromagnetic order in the multilayered structure. Such behavior clearly indicates that the ferromagnetism occurring in individual GaMnAs layers is truly long range. Furthermore, the reflectometry data reveal the spontaneous parallel alignment of the all GaMnAs layers' magnetizations that may result from the ferromagnetic interlayer coupling through nonmagnetic GaAs spacer [7].

Table 1 shows the calculated SLDs for the constituent materials of the superlattice for the

Table 1
Scattering length densities (SLD) for GaMnAs and GaAs for the NSF and SF neutron scattering processes in 10^{-6} Å^{-2} units

GaMnAs(++) N(b−p)	GaMnAs(−−) N(b+p)	GaMnAs(+−) Np	GaAs Nb
2.713	3.067	0.177	3.070

(++) and (−−) NSF reflectivities and the (+−) SF reflectivities. Due to the negative value of $b_{Mn} = -3.73$ fm and positive magnetic contribution from the 5/2 Mn spin, there is almost perfect compensation of the SLD contrast between GaMnAs and GaAs for the (−−) NSF reflectivity. Consequently, for this neutron spin direction, there should be no observable superlattice Bragg peak. For the other neutron polarization state, (++), the SL peak is enhanced compared with the unpolarized neutron experiment.

In Fig. 5 we present a detailed look at the first-order superlattice Bragg peak. The results of all the four NSF and SF reflection processes are displayed for experiments performed below and above T_C and in applied external fields of 2 and 100 G.

Above T_C (Fig. 5(c)), the sample is nonmagnetic (paramagnetic), and both (++) and (−−) cross sections coincide since only nuclear scattering is present. There is also no spin-flip scattering.

At 7.8 K and in 100 G external field (Fig. 5(b)), the sample is saturated and its magnetization is aligned parallel to the applied magnetic field. There is a SL Bragg peak in the (++) reflectivity and no such peak in the (−−) data, as one should expect according to the values of SLDs presented in Table 1. For the saturated sample, one should not expect any spin-flip scattering as there is no magnetization component perpendicular to the applied field.

The most important result for this specimen is presented in Fig. 5(a). The sample, after cooling down below T_C in zero external field, aligns spontaneously with its full moment and the direction of the sample magnetization is *reversed* compared to the situation depicted in Fig. 5(b) (the peak appears in (−−) NSF reflectivity). Thus, the observed alignment cannot be caused by the small

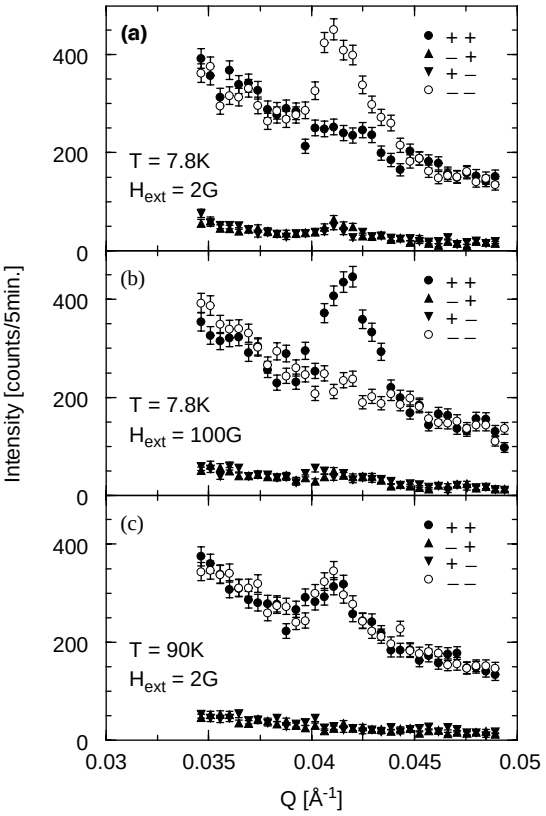

Fig. 5. Polarized neutron diffraction profiles about the first-order SL Bragg peak for (50 ML/6 ML) × 50 GaMnAs/GaAs superlattice. NSF reflection processes (++) and (−−) as well as SF ones (−+) and (+−) are presented. No peak in SF reflection indicates the absence of any component of the sample magnetization perpendicular to the applied guide field. Note the switch in the (++) and (−−) reflectivity (see (a) and (b)) after applying an external magnetic field of 100 G.

guide field (∼2 G) which has the same direction as the externally applied field. The height and the width of the SL peak are the same as for the sample saturated in an external field. Similarly, there is no spin-flip scattering present in this case. All these observations lead to the conclusion that each GaMnAs layer forms a single magnetic domain. Moreover, the magnetization of all layers is parallel, characteristic of ferromagnetically coupled superlattices. Our last conclusion about the interlayer coupling corroborates previous findings of IC in GaMnAs/GaAs trilayer systems [7] based on magnetization hysteresis loop analysis.

Acknowledgements

This work was supported by the projects NSF DMR-0204105 and KBN 2 P03B 154 18.

References

[1] S.A. Wolf, D.D. Awschalom, R.A. Buhrman, J.M. Daughton, S. von Molnar, M.L. Roukes, A.Y. Chtchelkanova, D.M. Treger, Science 294 (2001) 1488.
[2] T. Dietl, Semicond. Sci. Technol. 17 (2002) 377.
[3] H. Kepa, J. Kutner-Pielaszek, A. Twardowski, J. Blinowski, T. Story, P. Kacman, R.R. Galazka, K. Ha, H.J.M. Swagten, W.J.M. de Jonge, A.Yu. Sipatov, V. Volobuev, T.M. Giebultowicz, Europhys. Lett. 56 (2001) 54.
[4] J. Blinowski, P. Kacman, Phys. Rev. B 64 (2001) 045302.
[5] L.G. Parratt, Phys. Rev. 95 (1954) 359.
[6] H. Ohno, A. Shen, F. Matsukura, A. Oiwa, A. Endo, S. Katsumoto, Y. Iye, Appl. Phys. Lett. 69 (1996) 363.
[7] D. Chiba, N. Akiba, F. Matsukura, Y. Ohno, H. Ohno, Appl. Phys. Lett. 77 (2000) 1873.